J Bio Tribo Corros (2017) 3:24
DOI 10.1007/s40735-017-0084-1

Electrochemical Corrosion Characteristics of 439 Ferritic, 301 Austenitic, S32101 Duplex and 420 Martensitic Stainless Steel in Sulfuric Acid/NaCl Solution

Roland Tolulope Loto[1,2]

Received: 26 March 2017 / Revised: 31 March 2017 / Accepted: 7 April 2017

Abstract The corrosion behavior and pitting corrosion resistance of 439 ferritic, 301 austenitic, 420 martensitic and S32101 duplex stainless steel in 2 M H_2SO_4 at 0–1.5%NaCl concentrations were studied through potentiodynamic polarization measurement and optical microscopy analysis. Experimental observation shows that corrosion rate, pitting potential and passivation potential are influenced by the Cl^- ion concentration, alloy composition and metallurgical properties of the steels. 439 ferritic steel had significantly the lowest corrosion rate and highest pitting corrosion resistance. Surface morphology showed no visible change from comparison of steel samples before and after corrosion. The corrosion rates of the duplex steel were comparably lower than the austenitic and martensitic steel; however, it had the least pitting corrosion resistance with respect to Cl^- ion concentration. The martensitic steel despite quenching heat treatment for improved corrosion resistance had the highest corrosion rate values. The surface morphology of the steel samples except 439 ferritic steel showed the presence of micro- and macro-pits, and visible surface deterioration.

✉ Roland Tolulope Loto
tolu.loto@gmail.com

[1] Department of Mechanical Engineering, Covenant University, Ota, Ogun State, Nigeria

[2] Department of Chemical Metallurgical and Materials Engineering, Tshwane University of Technology, Pretoria, South Africa

Keywords Corrosion · Steel · Pitting · Passivation · Chloride

1 Introduction

Corrosion is responsible for plant shutdowns and accidents, costly design and maintenance, product contamination and wastage of valuable resources due to the aggressive nature of industrial environments on metallic surfaces of equipment and structures. Stainless steel corrosion is an electrochemical process, induced by certain electrolytic phenomena in interaction with corrosive environments. These steels are generally corrosion resistant and do perform optimally; however, the limit of their corrosion resistance depends on the composition of operating environment and strength of their passive protective films which itself is a product of the alloy composition and metallurgical structure. Formation and local breakdown of passive films on iron-based alloys has long been a subject of interest, reflecting the need for corrosion resistance of these metal materials [1, 2]. The passive film tends to break at some specific sites such as inclusions, grain boundaries and other discontinuities through which aggressive ions penetrate and initiate corrosion in the form of localized (pitting) attacks [3–5]. It is difficult to predict the incidence of pitting corrosion, particularly as the complexity of the corrosive environment increases and, even more so when fluctuations occur in the environmental parameters, as often arises in chemical processing plants. Pitting corrosion of metals is one of the most important electrochemical corrosion mechanisms, being a major cause of failure in different industrial media. Due to the localized nature of pitting corrosion, formation of pits is confined to much smaller areas compared to the total exposed surface [6].

Published online: 10 April 2017

Chloride ions have been known to destroy passivity or prevent its formation causing pit initiation. According to the autocatalytic mechanism of pitting corrosion, the pits become the anode of the redox process, while the surrounding metal substrate becomes the cathode accompanied by hydrolysis acidification of dissolved metallic ions and accumulation of diffused chloride ions [7]. Pitting potential, passivation potential, corrosion potential, etc., are some parameters used to evaluate pitting corrosion. The higher the pitting potential, the greater the pitting corrosion resistance of metallic alloys [8, 9]. Generally, the pitting potential decreases with increase in corrosion rate as chloride concentration increases. Many studies [10–12] have been done on corrosion and specifically pitting corrosion coupled with significant breakthrough on propagation mechanisms, environmental conditions and importance of electrochemical factors [13–15]. The mechanism of the pit initiation in relation to passive film deterioration is still debated. It is necessary to understand the relationship between the metallurgical structure, composition, surface morphology, corrosion resistance and pitting corrosion behavior of stainless steel alloys with extensive industrial applications to aid in material selection for effective corrosion control.

Steels such as martensitic stainless steel have been increasingly applied in oil and gas industries [16, 17]. 420 martensitic steel resists corrosion in industrial environments, in sea water, some dilute organic compounds, crude oil and gasoline, and other comparable corrosive media. Previous research has shown that quenching heat treatment improves the corrosion resistance of 420 martensitic steel by 60% [18]. 439 ferritic stainless steel is designed to resist corrosion in a variety of oxidizing conditions: in fresh water, boiling acids, heat exchanger tubing and hot water tanks as it provides good oxidation and corrosion resistance properties. 2101 duplex stainless steel is a low-nickel, lean duplex stainless steel designed with both superior strength and chloride stress-corrosion cracking resistance. It is used in applications such as chemical process pressure vessels, piping and heat exchangers, waste water handling systems, and desalination system chambers and evaporators. 301 austenitic stainless steel has corrosion resistance similar to that offered by 304. It is used as aircraft structural part and in a variety of industrial applications. The objective of this research is to study the corrosion resistance and pitting corrosion behavior of 439 ferritic, 301 austenitic, 321 duplex and 420 martensitic stainless steels in 2 M H_2SO_4 acid at specific concentrations of NaCl by means of potentiodynamic polarization measurements and optical microscopy analysis. Pitting potentials, corrosion potentials, passivation potentials, passivation range and corrosion currents were analyzed in each of the materials studied to assess their pitting corrosion resistance and passivation characteristics.

2 Experimental Methods

2.1 Materials and Preparation

439 ferritic (439SS), 301 austenitic (301SS), 321 duplex (321SS) and 420 martensitic (420SS) stainless steels sourced commercially had a nominal composition as shown in Table 1. The steel specimens after machining were abraded with silicon carbide papers (80, 320, 600, 800 and 1000) before washing with distilled water and propanone and kept in a desiccator for coupon analysis and potentiodynamic polarization test according to [19].

2.2 Potentiodynamic Polarization Technique

Polarization measurements were carried out at 30 °C using a three-electrode system and glass cell containing 200 mL of the corrosive test solution with Digi-Ivy 2311 electrochemical workstation. 2101SS and 301SS electrodes mounted in acrylic resin with an exposed surface area of 2.54 and 0.72 cm^2 were prepared according to [20]. Polarization plots were obtained at a scan rate of 0.0015 V/s between potentials of −0.5 and +1.5 V according to [21]. Platinum rod was used as the counter electrode and silver chloride electrode (Ag/AgCl) as the reference electrode. Corrosion current density (j_{cr}) and corrosion potential (E_{cr}) values were obtained using the Tafel extrapolation method. The corrosion rate (γ) and the inhibition efficiency (η_2, %) were calculated from the mathematical relationship:

$$C_R = \frac{0.00327 \times J_{corr} \times E_{qv}}{D} \quad (1)$$

j_{cr} is the current density in A/cm^2; D is the density in g/cm^3; E_{qv} is the sample equivalent weight in grams. 0.00327 is a constant for corrosion rate calculation in mm/y [22].

2.3 Optical Microscopy Characterization

Images of control and corroded 2101SS and 301SS surface morphology from optical microscopy were analyzed after weight-loss measurement with Omax trinocular through the aid of ToupCam analytical software.

3 Result and Discussion

3.1 Electrochemical Analysis

The potentiodynamic polarization curves of 420SS, 439SS, 321SS and 301SS samples in 2 M H_2SO_4 at specific Cl^- ion concentrations of 0–1.5% are shown in Figs. 1, 2, 3 and 4. Table 2 depicts the results from the polarization curves.

Table 1 Percentage nominal composition of 439SS, 301SS, 321SS and 420SS

Element symbol	Cu	Si	Br	Ni	Cr	Mn	P	S	C	Mo	Fe
% composition (439SS)	–	0.75	–	0.5	19	0.5	–	–	0.025	–	79.23
% composition (301SS)	–	1	–	8	16	2	0.045	0.03	0.15	–	72.80
% composition (321SS)	0.8	1.6	1.2	1.5	22.8	–	0.04	0.03	0.04	0.9	71.09
% composition (420SS)	–	1	–	–	13	0.8	0.04	0.03	0.15	–	84.98

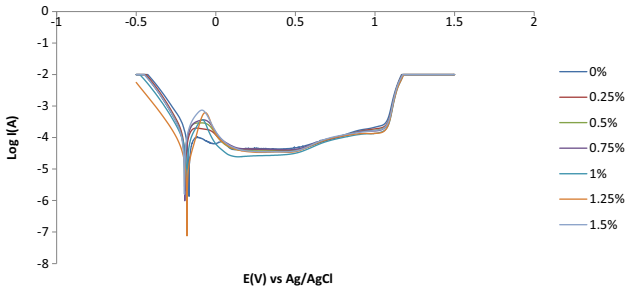

Fig. 1 Potentiodynamic polarization curves of 439SS in 2 M H_2SO_4 at 0–1.5%NaCl

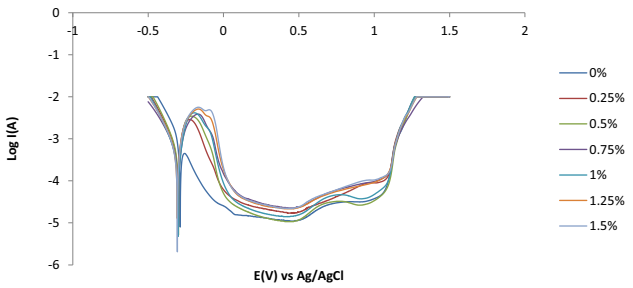

Fig. 2 Potentiodynamic polarization curves of 301SS in 2 M H_2SO_4 at 0–1.5%NaCl

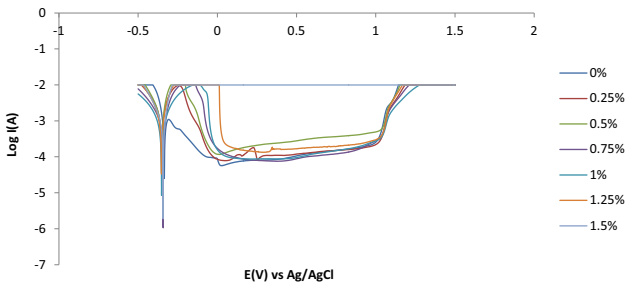

Fig. 3 Potentiodynamic polarization curves of 321SS in 2 M H_2SO_4 at 0–1.5%NaCl

The curves show typical anodic polarization behavior of stainless steels in a NaCl solution consisting of active dissolution, passivation and progressive increase in the corrosion due to pitting. 420SS and 439SS samples showed uniform polarization behavior over the potential domain at all Cl^- ion concentrations in comparison with 321SS, and 301SS after 0%NaCl. Observation of the corrosion rate values of the steel samples shows that 439SS has the lowest corrosion rates, while 420SS has the highest values. This

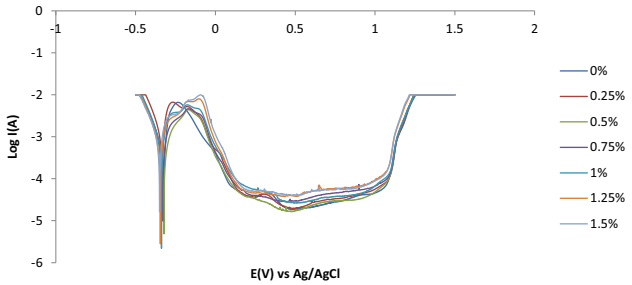

Fig. 4 Potentiodynamic polarization curves of 420SS in 2 M H_2SO_4 at 0–1.5%NaCl

coincides with the visibly low corrosion potential values of 439SS at an average potential of −0.191 V after 0%NaCl, corresponding to strong resistance to anodic dissolution. Its polarization resistance values confirm the observation showing the highest figures among the steel samples. 420SS and 321SS showed very high corrosion potential values followed by 301SS; however, the corrosion rate and polarization resistance values of 321SS are relatively low signifying active polarization and redox electrochemical mechanisms occurring at the metal–solution interface of the sample. Changes in Cl^- ion concentration had a significant influence on the corrosion rate values of the tested steel samples with the exception of 439SS. Increase in salt concentration caused a proportionate increase in the corrosion rate of 321SS and 301SS which peaked at 0.5%NaCl before decreasing minimally till 1.5%NaCl. 420SS experienced a decrease in corrosion rate with increase in NaCl concentration till 0.75%NaCl after which it increased till 1.5%NaCl. These observations show that stainless steel grades respond differently to Cl^- ion concentration due to differences in their metallurgical structure, heat treatment process and chromium content.

It also shows that changes in Cl^- ion concentration have significant influence on the polarization behavior of the stainless steel grades and hence its penetration of their passive film. The steel grades apart from 420SS showed consistent active–passive behavior from 0.25 to 1.5%NaCl. After 0%NaCl, 420SS shifted consistently to anodic polarization potentials signifying increased redox electrochemical processes responsible for greater surface deterioration of the steel. At 0.5%NaCl, 439SS had a peak anodic–cathodic current (E_{corr}) of 2.81E−6/−0.200 $V_{Ag/AgCl}$ after a consistent increase from 0%NaCl after which it

Table 2 Polarization results for 439SS, 301SS, 420SS and 321SS in 2 M H_2SO_4 at 0–1.25%NaCl

Sample	NaCl conc. (%)	Corrosion rate (mm/y)	Corrosion current (A)	Corrosion current density (A/cm^2)	Corrosion potential (V)	Polarization resistance, R_p (Ω)	Cathodic potential, B_c	Anodic potential, B_a
439SS								
A	0	0.81	1.13E−04	7.51E−05	−0.168	228.20	−7.632	−1.94
B	0.25	1.04	1.45E−04	9.69E−05	−0.191	176.90	−8.907	−0.28
C	0.5	1.13	1.58E−04	1.06E−04	−0.196	162.20	−8.807	0.68
D	0.75	1.04	1.46E−04	9.71E−05	−0.195	176.30	−9.065	2.19
E	1	0.62	8.60E−05	5.73E−05	−0.183	298.80	−8.932	7.47
F	1.25	0.20	2.78E−05	1.86E−05	−0.181	922.80	−9.111	17.47
G	1.5	1.09	1.53E−04	1.02E−04	−0.197	168.50	−9.288	6.12
301SS								
A	0	14.74	8.48E−04	1.41E−03	−0.287	30.29	−7.11	−7.69
B	0.25	14.98	8.62E−04	1.44E−03	−0.302	29.79	−7.82	0.50
C	0.5	15.51	8.93E−04	1.49E−03	−0.299	30.13	−8.28	1.57
D	0.75	10.51	6.05E−04	1.01E−03	−0.300	42.46	−7.32	5.54
E	1	10.52	6.06E−04	1.01E−03	−0.301	46.23	−8.45	5.29
F	1.25	11.20	6.45E−04	1.07E−03	−0.307	36.46	−7.59	5.33
G	1.5	11.46	6.60E−04	1.10E−03	−0.306	38.94	−7.89	5.89
420SS								
A	0	15.32	1.10E−03	1.40E−03	−0.324	23.28	−9.655	2.98
B	0.25	12.80	9.23E−04	1.17E−03	−0.330	26.54	−9.463	3.12
C	0.5	12.51	9.02E−04	1.14E−03	−0.323	40.02	−9.551	4.85
D	0.75	12.16	8.77E−04	1.11E−03	−0.331	29.31	−8.833	3.19
E	1	15.44	1.11E−03	1.41E−03	−0.338	21.54	−9.363	1.12
F	1.25	16.31	1.18E−03	1.49E−03	−0.345	23.65	−9.639	2.21
G	1.5	16.63	1.20E−03	1.52E−03	−0.350	19.79	−8.117	1.51
321SS								
A	0	8.28	1.95E−03	7.69E−04	−0.335	13.15	−2.678	−2.62
B	0.25	9.72	2.30E−03	9.04E−04	−0.352	11.19	−6.267	4.92
C	0.5	10.75	2.54E−03	9.99E−04	−0.352	10.13	−7.878	0.00
D	0.75	6.10	1.44E−03	5.67E−04	−0.342	17.83	−6.614	6.14
E	1	4.32	1.02E−03	4.01E−04	−0.352	25.21	−6.082	6.68
F	1.25	7.73	1.83E−03	7.19E−04	−0.352	14.07	−7.494	4.75
G	1.5	7.95	1.88E−03	7.39E−04	−0.342	15.32	−8.507	0.00

declined progressively till 1.5%NaCl. This observation contrasts what was observed for the other steel samples as changes in Cl^- ion concentration caused differential changes in peak current values.

3.2 Pitting Corrosion Evaluation

The pitting mechanisms of the four stainless steels alloys are related to the collapse of their passive protective film, which itself is a product of their alloy composition and structure. The steels underwent stable pitting after the pitting potentials (E_{pit}, Figs. 1, 2, 3, 4, Table 3). Once pitting occurred, breakdown of passive film and active dissolution of the metal substrate cause changes in the electrochemical characteristics of oxide film The E_{pit} for quenched 420SS and 321SS increased with increase in Cl^- ion concentration and peaked at 0.5%NaCl for 420SS coupled with a corresponding increase in current at E_{pit} and 0.75%NaCl for 321SS without a proportionate change in current at E_{pit}. These observations show that the passive films of the two alloys respond to changes in Cl^- ion concentration before breakage and the onset of stable pitting. Their resistance to pitting corrosion increases until a peak value after which they remain unaffected with changes in Cl^- ion concentration signifying a threshold Cl^- ion concentration beyond which pitting potential does not

Table 3 Potentiostatic data of pitting and passivation potentials for 439SS, 301SS, 420SS and 321SS in 2 M H_2SO_4 at 0–1.5%NaCl

Sample	NaCl conc. (%)	Pitting potential (V), E_{pit}	Current at E_{pit} (A)	Passivation potential (V), E_{pp}	Current at E_{pp} (A)	Passivation range (V)
439SS						
A	0	1.00	2.10E−04	−0.19	1.35E−04	1.19
B	0.25	1.00	1.88E−04	−0.11	1.98E−04	1.11
C	0.5	1.00	1.70E−04	−0.12	2.88E−04	1.12
D	0.75	0.99	1.62E−04	−0.12	3.16E−04	1.11
E	1	0.99	1.32E−04	−0.11	2.91E−04	1.10
F	1.25	0.99	1.34E−04	−0.10	3.44E−04	1.09
G	1.5	0.99	1.64E−04	−0.12	5.38E−04	1.11
301SS						
A	0	1.06	4.93E−05	−0.30	6.70E−04	1.36
B	0.25	1.04	9.39E−05	−0.26	2.24E−03	1.30
C	0.5	1.03	3.92E−05	−0.25	2.51E−03	1.28
D	0.75	1.03	1.04E−04	−0.23	2.62E−03	1.26
E	1	1.02	5.21E−05	−0.23	3.14E−03	1.25
F	1.25	1.02	9.81E−05	−0.22	3.72E−03	1.24
G	1.5	1.03	1.11E−04	−0.16	5.51E−03	1.19
420SS						
A	0	1.00	4.59E−05	−0.27	4.68E−03	1.27
B	0.25	1.01	5.78E−05	−0.26	6.09E−03	1.27
C	0.5	1.04	6.11E−05	−0.20	3.39E−03	1.24
D	0.75	1.05	8.45E−05	−0.19	3.91E−03	1.24
E	1	1.05	9.72E−05	−0.18	5.72E−03	1.23
F	1.25	1.05	1.23E−04	−0.18	6.78E−03	1.23
G	1.5	1.05	1.16E−04	−0.13	8.07E−03	1.18
321SS						
A	0	0.91	1.86E−04	−0.33	5.25E−04	1.24
B	0.25	0.94	1.86E−04	−0.29	7.02E−04	1.23
C	0.5	0.95	4.52E−04	−0.27	9.94E−03	1.22
D	0.75	0.99	2.26E−04	−0.21	9.94E−03	1.20
E	1	0.99	2.64E−04	−0.17	9.29E−03	1.16
F	1.25	0.97	2.77E−04	−0.04	9.94E−03	1.01
G	1.5	0	0	0	0	0

change. At 1.5%NaCl, 321SS shows no passivity resulting in nil pitting potential. At this Cl^- ion concentration, the steel's passivity was completely destroyed. The pitting potential values for 301SS decreased with increase in Cl^- ion concentration showing that the pitting resistance; hence, the strength of its passive film decreases in response to changes in Cl^- ion concentration leading to the initiation and propagation of corrosion pits. Due to the anodic reactions within the pitted regions of the 301SS and the reduction reaction on the passive metal surface surrounding the pit, the charge neutrality of the pit electrolyte results in the accumulation of Cl^- ions in response to the release of metal cations within the electrolyte [23, 24]. Penetration of Cl^- ions through the passive film at sites of inclusions and breakage of the film is suggested through which the Cl^- ions reach the metal substrate. Previous research has shown that pitting initiates from flaws in the oxide film and propagates by the ion transport mechanism [25]. The film is further weakened by the resulting cationic and oxygen vacancies leading to dissolution of the steel [26–28]. The pitting potential of 439SS remained unchanged with respect to Cl^- ion concentration coupled with a consistent decrease in current at E_{pit}. Previous discussion showed that it has a very low corrosion rate at passive corrosion potentials. The observation from the pitting potential values shows its passive film to be highly resistant to

oxidation and Cl^- ion penetration at high electric potentials. Pitting corrosion being the local break in the passive layer of the stainless steel provoked by the presence of Cl^- ions in the acid solution, it is obvious that the potential of 439SS in the acid chloride solution is inferior to the pitting potential.

3.3 Metastable Pitting and Passivity

The passive film formed on the stainless steel surfaces enforces controlled equilibrium of ionic transport through it. The film consists basically of chromium oxides, hydroxides and iron compounds, which form at the metal–solution interface. Under induced potential, the passivation characteristics of stainless steel alloys become dynamic with respect to scan rate and Cl^- ion concentration in the acid media. The passivation behavior of 420SS, 321SS and 301SS followed a similar trend as shown in Table 3; it is observed that increase in Cl^- ion concentration results in proportionate decrease in passivation potentials of the alloys indicating a decrease in their overall pitting resistance with respect to solution concentration as a result of metastable pitting activity. This is confirmed from the passivation range values (Table 3) which showed a visible decrease in potential. Cl^- ions are known to be aggressive enough to attack steel and initiate pitting. Their small size facilitates diffusion which enhances electrical neutrality and hydrolysis of the corrosion products within the pits causing acidification, and hence hindering passivation. The passivation current for aforementioned steels increased with decrease in passivation potential which eventually leads to a progressive increase in the metastable region of their polarization curves, an indication that the passive film is undergoing localized but transient pitting due to temporary breakdown of the passive film, and the creation and growth of small, occluded cavities before stable passivation. With increase in Cl^- ion concentration, the anodic dissolution rate and the lifetime of the metastable pit increase resulting in higher metastable pitting nucleation rate before passivation. Due to local Cl^- ions enrichment, current transients were observed for 420SS at the passive regions probably at the active sites on surface such as inclusions, crystal boundaries, dislocations and irregularities, resulting in damage of passive film and limited dissolution of the substrate metal.

The passivation behavior of 439SS with respect to potential contrasts the observation for the three earlier discussed steels. Results show that Cl^- ion concentration has no effect on its passivation potential after 0%NaCl. It is obvious that there is a significant difference between nil Cl^- ion concentration and specific addition of NaCl to the solution. After 0%NaCl, the passivation potential remained generally the same; however, the passivation current increased with Cl^- ion concentration signifying increase in metastable pitting activity, but at relatively lower passivation current hence higher pitting resistance in comparison with other alloys. 321SS had a potential of −0.29 V, while the value for 420SS and 301SS is −0.14 V when we consider the difference between the passivation potential value at 0 and 1.5%NaCl. Comparing their values to 439SS at −0.07 V, it is clearly seen that the passivation characteristics and pitting corrosion resistance of 439SS are significantly superior to the other steels.

3.4 Surface Morphology Analysis

The optical images of the stainless steel samples before and after the potentiodynamic polarization test are shown in Figs. 5a, b, 6a, b, 7a, b and 8a, b. 439SS (Fig. 5a, b) which shows no visible morphological deterioration from the action of Cl^- ions during potential scanning. The surface characteristics remained virtually unchanged in comparison with the other steels. This observation confirms the results on corrosion rate, pitting potential and passivation behavior. Obviously, the transfer or adsorption of Cl^- ions through the passive layer to the metal surface where they start their specific action was limited. Studying the morphology of the other steel (301SS, 321SS and 420SS), there is a clear contrast between the samples before and after polarization. 301SS and 321SS showed portions of mild to severe surface deterioration with the appearance of a number of macro-pits. The electrochemical action of the Cl^- ions weakened the passive film, causing an enhanced dissolution of the alloy surface. The grain boundary on 321SS appeared faintly compared to 420SS where coarse grain boundary due to quenching heat treatment is clearly visible with insidious pits on the surface.

4 Conclusion

The effect of Cl^- ion concentration on 439SS, 301SS, quenched heat-treated 420SS and 2101SS in 2 M H_2SO_4 gave mixed results for corrosion rate, pitting corrosion resistance and passivation characteristics; 439SS showed significantly higher corrosion and pitting resistance compared to other steels. Changes in Cl^- ion concentration had no influence on its electrochemical characteristics. S32101 duplex steel with its austenite ferrite microstructure had a comparably better corrosion resistance than 301SS and 420SS, but displayed lower pitting resistance due to more active polarization on its surface. Cl^- ion concentration had limited influence on the corrosion rates of the steels as compared to the pitting corrosion where it had a significantly higher influence. Surface morphology of 439SS remained unchanged compared to others which showed

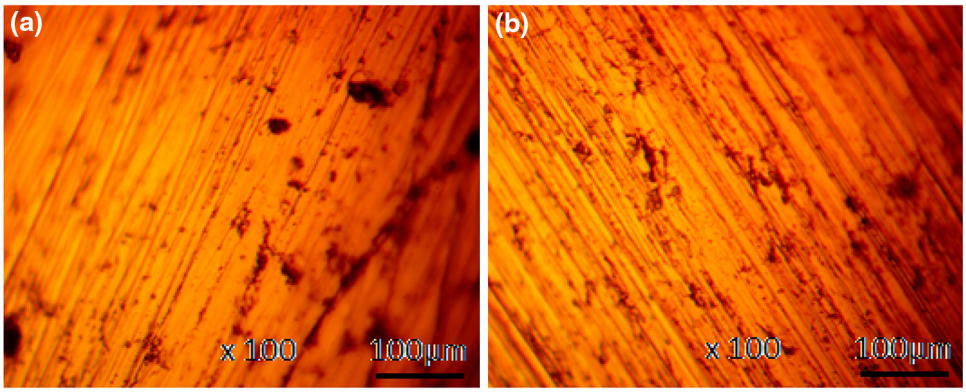

Fig. 5 Optical image of 439SS at mag. ×100 **a** before corrosion, **b** after corrosion

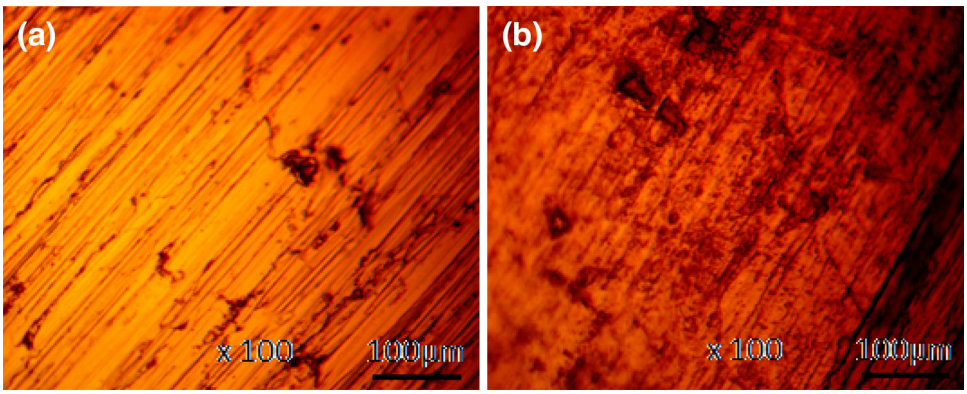

Fig. 6 Optical image of 301SS at mag. ×100 **a** before corrosion, **b** after corrosion

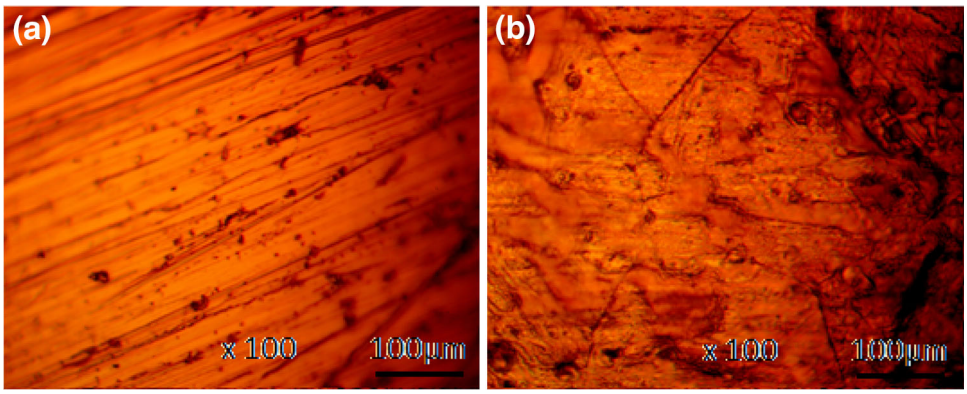

Fig. 7 Optical image of 321SS at mag. ×100 **a** before corrosion, **b** after corrosion

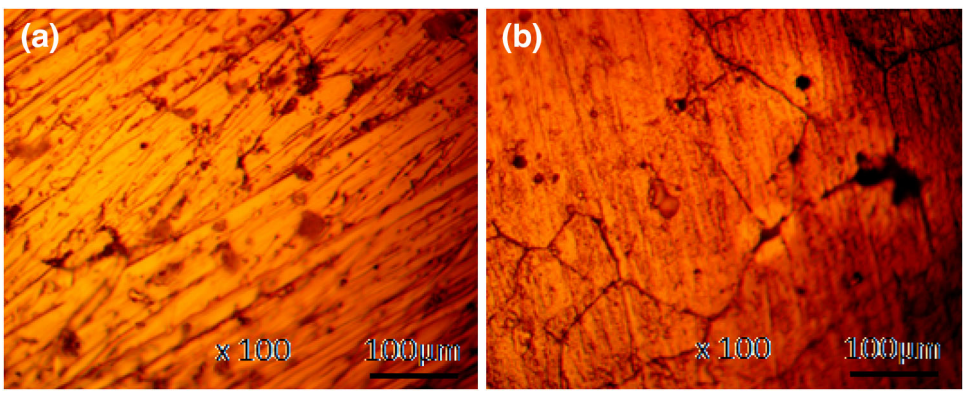

Fig. 8 Optical image of 420SS at mag. ×100 **a** before corrosion, **b** after corrosion

progressive deterioration and the formation of visible micro- and macro-pits.

Acknowledgements The author is grateful to Covenant University, Ota, Ogun State, Nigeria for the funding of the research and provision of research facilities.

Compliance with Ethical Standards

Conflict of interest Author declare no conflict of interest.

References

1. Guo LQ, Lin MC, Qiao LJ, Volinsky AA (2014) Duplex stainless steel passive film electrical properties studied by in situ current sensing atomic force microscopy. Corros Sci 78:55–62. doi:10.1016/j.corsci.2013.08.031
2. Fredriksson W, Malmgren S, Gustafsson T, Gorgoi M, Edström K (2012) Full depth profile of passive films on 316L stainless steel based on high resolution HAXPES in combination with ARXPS. Appl Surf Sci 258(15):5790–5797. doi:10.1016/j.apsusc.2012.02.099
3. Williams DE, Kilburn R, Cliff J, Waterhouse GIN (2010) Composition changes around sulphide inclusions in stainless steels, and implications for the initiation of pitting corrosion. Corros Sci 52(11):3702–3716. doi:10.1016/j.corsci.2010.07.021
4. Williams DE, Stewart J, Balkwill PH (1994) The nucleation, growth and stability of micropits in stainless steel. Corros Sci 36(7):1213–1235. doi:10.1016/0010-938X(94)90145-7
5. Paroni ASM, Alonso-Falleiros Magnabosco R (2006) Sensitization and pittingcorrosion resistance of ferritic stainless steel aged at 800 °C. Corrosion 62(11):1039–1046. doi:10.5006/1.3278231
6. Munoz AI, Anton JG, Nuevalos SL, Guinon JL, Herranz VP (2004) Corrosion studies of austenitic and duplex stainless steels in aqueous lithium bromide solution at different temperatures. Corros Sci 46(12):2955–2974. doi:10.1016/j.corsci.2004.05.025
7. Gan Y, Li Y, Lin HC (2001) Experimental studies on the local corrosion of low alloy steels in 3.5% NaCl. Corros Sci 43(3):397–411. doi:10.1016/S0010-938X(00)00090-1
8. Revie RW, Uhlig HH (2008) Corrosion and corrosion control. Wiley, New York. doi:10.1002/bbpc.19630670926
9. Moayed MH, Newman RC (2006) Evolution of current transients and morphology of metastable and stable pitting on stainless steel near the critical pitting temperature. Corros Sci 48(4):1004–1018
10. Pistorius PC, Burstein GT (1992) Metastable pitting corrosion of stainless steel and the transition to stability. Philos Trans Phys Sci Eng 341(1662):531–559. doi:10.1098/rsta.1992.0114
11. Pistorius PC, Burstein GT (1992) Growth of corrosion pits on stainless steel in chloride solution containing dilute sulphate. Corros Sci 33(12):1885–1897. doi:10.1016/0010-938X(92)90191-5
12. Ernst P, Laycock NJ, Moayed MH, Newman RC (1997) The mechanism of lacy cover formation in pitting. Corros Sci 39(6):1133–1136. doi:10.1016/S0010-938X(97)00043-7
13. Ramezanzadeha B, Niroumandradb S, Ahmadib A, Mahdaviana M, Moghadam Mohamadzadeh MH (2016) Enhancement of barrier and corrosion protection performance of an epoxy coating through wet transfer of amino functionalized graphene oxide. Corros Sci 103:283–304. doi:10.1016/j.corsci.2015.11.033
14. Nianwei D, Lai-Chang Z, Junxi Z, Qimeng C, Maoliang W (2016) Corrosion behaviour of selective laser melted Ti-6Al-4 V alloy in NaCl solution. Corros Sci 102:484–489
15. Samira N, Babak J, Ali E (2015) Electrophoretic deposition of graphene oxide on aluminum: characterization, low thermal annealing, surface and anticorrosive properties. Bull Chem Soc Jpn 88(5):722–728. doi:10.1246/bcsj.20140402
16. Marchebois H, Leyer J, Orlans-Joliet B (2007) SCC performance of a super 13Cr martensitic stainless steel for OCTG: three-dimensional fitness-for-purpose mapping according to PH2S, pH and chloride content. In: NACE corrosion conference. NACE International Houston
17. Li X, Bell T (2006) Corrosion properties of plasma nitrided AISI 410 martensitic stainless steel in 3.5% NaCl and 1% HCl aqueous solutions. Corros Sci 48(8):2036–2049. doi:10.1016/j.corsci.2005.08.011
18. Loto RT, Aiguwurhuo O, Evana U (2016) Corrosion resistance study of heat treated 420 martensitic stainless steel and 316 austenitic stainless steel in dilute acid concentrations. Rev Téc Ing Univ Zulia 39(7):35–40. doi:10.21311/001.39.7.04
19. ASTM G1-03 (2011) Standard practice for preparing, cleaning, and evaluating corrosion test specimens. http://www.astm.org/Standards/G1. Retrieved 30 May 2016
20. ASTM G59-97 (2014) Standard test method for conducting potentiodynamic polarization resistance measurements. http://www.astm.org/Standards/G31. Retrieved 30 May 2016
21. ASTM G102-89(2015)e1 Standard practice for calculation of corrosion rates and related information from electrochemical measurements. http://www.astm.org/Standards/G31. Retrieved 30 May 2016
22. Choi YS, Nesic S, Ling S (2011) Effect of H_2S on the CO_2 corrosion of carbon steel in acidic solutions. Electrochim Acta 56(4):1752–1760. doi:10.1016/j.electacta.2010.08.049
23. Burstein GT, Mattin SP (1992) Nucleation of corrosion pits on stainless steel. Philos Mag Lett 66(1–4):127–131. doi:10.1016/0010-938X(93)90133-2
24. Burstein GT, Vines SP (2001) Repetitive nucleation of corrosion pits on stainless steel and the effects of surface roughness. J Electrochem Soc 148(12):B504–B516. doi:10.1149/1.1416503
25. Wood GC, Richardson JA, Abd Rabbo MF, Mapa LB, Sutton WH (1978) The role of flaws in breakdown of passivity of aluminum and crevice corrosion of stainless steel. In: Frankenthal RP, Kruger J (eds) Passivity of metals, the electrochemical society. Princeton University Press, Princeton, pp 973–988
26. Frankel GS (1998) Pitting corrosion of metals: a review of the critical factors. J Electrochem Soc 145(6):2186–2198. doi:10.1149/1.1838615
27. Sato N (1971) A theory for breakdown of anodic oxide films on metals. Electrochim Acta 16(10):1683–1692. doi:10.1016/0013-4686(71)85079-X
28. Sato N, Kudo K, Noda T (1971) The anodic oxide film on iron in neutral solution. Electrochim Acta 16(11):1909–1921. doi:10.1016/0013-4686(71)85146-0